Available online at www.sciencedirect.com
SCIENCE DIRECT®
European Journal of Medicinal Chemistry 41 (2006) 373–378
EUROPEAN JOURNAL OF MEDICINAL CHEMISTRY
http://france.elsevier.com/direct/ejmech

Original article

3D QSAR for GSK-3β inhibition by indirubin analogues

Na Zhang [a], Yongjun Jiang [b,*], Jianwei Zou [b], Bing Zhang [a], Haixiao Jin [a], Yanhua Wang [a], Qingsen Yu [a,b]

[a] *Department of Chemistry, Zhejiang University, 310027 Hangzhou, Zhejiang Province, China*
[b] *Key Laboratory for Molecular Design and Nutrition Engineering of Ningbo City, Ningbo Institute of Technology, Zhejiang University, 315100 Ningbo, Zhejiang Province, China*

Received 23 May 2005; received in revised form 20 October 2005; accepted 26 October 2005
Available online 25 January 2006

Abstract

Glycogen synthase kinase 3 (GSK-3) plays an important role in a diverse number of regulatory pathways by phosphorylation of several different cellular targets and its inhibitors have been evaluated as promising drug candidates. Indirubin analogues show favorable inhibitory activity targeting GSK-3β, which is closely related to the property and position of substituents. Two methods were used to build 3D-QSAR models for indirubin derivatives. The conventional 3D-QSAR (ligand-based) studies were performed based on the lower energy conformations employing atom fit alignment rule. The receptor-based 3D-QSAR models were also derived using bioactive conformations obtained by docking the compounds to the active site of GSK-3. Conclusions of models based on two methods are similar and reliable. The results indicate that both ligand-based and receptor-based are feasible tools to build 3D-QSAR models. Contour maps of the receptor-based CoMSIA model ($q^2 = 0.766$, $r^2 = 0.908$, N (number of components) = 5) including the steric, electronic and hydrophobic fields were taken as representative to explain factors affecting activities of inhibitors.

Keywords: GSK-3β; Indirubins; Molecular docking; 3D QSAR; CoMFA; CoMSIA

1. Introduction

Glycogen synthase kinase 3 (GSK-3) is a cytosolic serine/threonine protein kinase found in two closely related isforms, GSK-3α and GSK-3β, which are expressed ubiquitously in mammalian tissues [1]. Both isoforms have nearly identical biochemical functions and substrate affinities, sharing a sequence identity of some 95% in the catalytic domain [2]. Recent reviews give a more detailed description of the roles GSK-3 plays in the different cellular pathways including cell differentiation, cellular growth and proliferation, metabolic processes, apoptosis control, and mechanisms involved in neuronal function [3,4]. Consequently, GSK-3 could be regarded as a potential therapeutic target and its small molecule inhibitors may have a therapeutic potential in numerous human diseases such as cancer, type 2 diabetes and neurological diseases such as bipolar disorders or Alzheimer's disease [5,6].

Structure–activity relationship studies define some structural requirements for potency of inhibitors. And the 3D-QSAR studies of pallones [7], maleimides [8], and aloisines [9] have been reported. Indirubin is an active ingredient of Danggui Longhui Wan, a traditional Chinese medicine recipe used to treat chronic diseases such as leukemias [10]. A variety of indirubins were identified as powerful inhibitors of GSK-3 while other structurally related indigoids were inactive [11]. It is noteworthy that indirubin's analogues such as indiribin-3′-oxime, 5-chloro-indirubin etc. show better pharmacological effect and less toxicity than those of indirubin. The biological activities are closely related to substituents' property and position of indirubins. However, there is no relevant study concerning QSAR studies of indirubin derivates presently, relationships between structures and activities of indirubins could guide us to understand their pharmacological mechanism and design more favorable inhibitors.

* Corresponding author. Tel.: +86 574 8822 9517; fax: +86 574-8822 9516.
E-mail address: yjjiang@nit.net.cn (Y. Jiang).

0223-5234/$ - see front matter © 2006 Elsevier SAS. All rights reserved.
doi:10.1016/j.ejmech.2005.10.018

In 3D-QSAR studies, molecular conformations and alignment rules are usually one of key steps for the meaningful results. Molecular docking is an attractive way to get putative bioactive conformations for building 3D-QSAR models, and several applications of docking alignment have been reported in [12–14]. In this paper, lower energy conformation with atom fit alignment and docking conformation are applied to seek the structure–activity relationship of indirubins. Further, we will focus on the models based on docking conformation to explore the favorable or unfavorable factors affecting the inhibitory activity.

2. Methods

2.1. Molecules preparation

From available series of 42 compounds, a training set and a test set including, respectively, **34** and **8** compounds have been selected randomly. The geometries of molecules except indirubin-3′-oxime (No. 16, directly extracted from PDB ID: 1Q41) were constructed using BioMedCache version 6.0 [15] with AM1 method to obtain lower energy conformations. Gasteiger–Hückel charges were assigned on inhibitors by the software package Sybyl6.8 [16]. The structures and experimental activities ($pIC_{50} = -\log_{10}{}^{IC}{}_{50}$) are listed in Table 1 [17] (the test set with asterisk).

2.2. Molecular modeling

Computational docking was performed using Sybyl 6.8 and Autodock3.05 [18]. To explore the best orientations of substituents, inhibitors were docked into the active site of GSK-3β. The crystal structure of indirubin-3′-oxime complexed with GSK-3β taken from the protein data bank (PDB ID:1Q41) was used to optimize docking parameters and test the docking quality achieved by Audock3.05. Firstly, lost residues of GSK-3β were added by loop search method of Sybyl 6.8. GSK-3β was checked for polar hydrogens and assigned for partial atomic charges, the PDBQs file was created, and the atomic solvation parameters were also assigned for the macromolecule. The torsion angles of inhibitors were defined in order to explore conformations during the process of docking. Secondly, the 3D-grid maps with grid spacing 0.375 Å and $60 \times 60 \times 60$ points were created by the AutoGrid algorithm to evaluate the binding energies between the inhibitors and the GSK-3. During docking processes, the number of generations, energy evaluations, and docking runs were set to 370,000, 1500,000 and 10, respectively. Finally, the best docking conformation of each inhibitor was selected according to the criteria of interacting energy combined with geometrical matching quality for 3D-QSAR studies. Then, other cases were docked sequentially into the binding pocket of GSK-3β using the parameters previously optimized.

2.3. CoMFA and CoMSIA 3D QSAR models

CoMFA and CoMSIA studies require the bioactive conformations and suitable alignment rule. Receptor-based method means the best conformations of all inhibitors except No. 16 (bioactive conformation extracted from 1Q41) clustering in the binding pocket of receptor obtained from molecular docking were directly used to build models. For ligand-based method, the lower energy conformations of inhibitors were superimposed to alignment template compound **16**, indirubin-3-oxime in the crystal complex of 1Q41, reference atoms are four rings almost in one plane and the oxygen atom shown in Table 1.

The CoMFA steric and electostatic fields were calculated at grid points using the Lennard–Jones and coulomb potential functions of the tripos field with a default energy cutoff, 30 kcal mol^{-1}. An sp^3 carbon atom with a charge of + 1.0 and a VDW radius of 1.52 Å was probed on 2 Å spaced lattice, which extended 4 Å units beyond the dimensions of aligned molecules in all directions. For CoMSIA, steric, electrostatic and hydrophobic three field descriptors among the five field descriptors (steric, electrostatic, hydrophobic, hydrogen bond donor and acceptor) were evaluated using the probe atom with + 1 charge, radius of 1 Å and + 1 hydrophobicity on the same lattice as the CoMFA used, since the additions of hydrogen bond donor and acceptor fields in CoMSIA model do not significantly improve the model.

PLS regression analysis was used to explore a linear relationship between field descriptors (as independent variables) and biological activities (pIC_{50} as dependent variables). The leave-one-out (LOO) and leave-some-out (LSO, 10 groups) cross-validation with 2 kcal mol^{-1} column filtering were performed to determine optimum number of components and cross-validated coefficient q^2, which indicates the consistency and predictiveness of models. Then, non-cross-validation was performed to derive the final PLS regression models.

3. Results and discussion

3.1. Molecular docking

One angstrom RMS deviation between the docked and crystal structure of indirubin-3′-oxime (Fig. 1), as well as the hydrogen bonds predicted by molecular docking just like those in the crystal structure validates the reliability of these docking parameters. The crystal structure of indirubin-3′-oxime complexed with GSK-3β shows some characteristic of binding pocket [19] divided into three parts. The pocket sandwiches the inhibitor between Ile62, Val70, and Ala83 on the top and Leu188 on the bottom. The hinge segment is formed using the chain of Leu132-Asp133-Tyr134-Val135-Pro136. There are three hydrogen bonds involved Asp133 and Val135 with indirubin-3′-oxime. The N1 atom of the inhibitor, as the donor, forms a hydrogen bond with the carbonyl oxygen of Asp133. The backbone nitrogen and carbonyl oxygen of Val 135 are involved to form the other two hydrogen bonds with O2 and

Table 1
Structures, experimental activity (EA pIC_{50}) vs. predicted activity (PA pIC_{50}) and residuals by CoMFA and CoMSIA of 42 compounds (test set with asterisk)

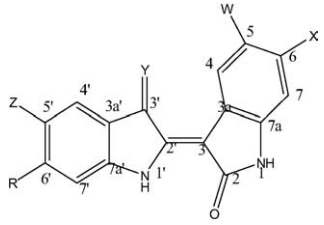

Number	Y	W	X	Z	R	EA	CoMFA PA	CoMSIA PA	Residuals CoMFA	Residuals CoMSIA
01	O				Br	6.00	6.30	6.59	–0.30	–0.59
02	O	CH_3			Br	7.20	7.04	6.82	0.16	0.38
03	O	Cl			Br	7.30	7.15	7.00	0.15	0.30
04	O	Br			Br	7.26	6.95	7.07	0.31	0.19
05	O			Br		6.46	6.15	6.20	0.31	0.26
06	O		$CH{=}CH_2$			6.62	6.28	6.38	0.34	0.24
07	O		F			6.19	6.34	6.47	–0.15	–0.28
08	O		Cl			6.85	6.81	6.79	0.04	0.06
09	O		I			7.26	7.08	7.37	0.18	–0.11
10	O				Br	4.66	4.94	4.80	–0.28	–0.14
11	O	B_r		B_r		6.60	6.75	6.84	–0.15	–0.24
12	O		Br		Br	5.35	5.77	5.73	–0.42	–0.38
13	O	Cl	Cl			7.52	7.20	7.46	0.32	0.06
14	O	NO_2	Br			7.00	7.47	7.02	–0.47	–0.02
15	O	CH_3	Br			7.60	7.48	7.52	0.12	0.08
16	NOH					7.66	7.53	7.62	0.13	0.04
17	NOH	I				8.05	8.36	8.29	–0.31	–0.24
18	NOH		$CH{=}CH_2$			7.22	7.64	7.34	–0.42	–0.12
19	NOH		Cl			7.70	7.59	7.45	0.11	0.25
20	NOH		Br			8.30	8.04	7.99	0.26	0.31
21	NOH					8.00	7.87	8.00	0.13	0.00
22	NOH				Br	6.47	6.17	5.99	0.30	0.48
23	O	I				7.17	7.17	7.38	0.00	–0.21
24	NOH		Br		Br	6.92	6.53	6.59	0.39	0.33
25	NOH	NO_2	Br			8.15	8.32	8.20	–0.17	–0.05
26	$NOCH_3$					6.82	6.76	6.72	0.06	0.10
27	$NOCH_3$		Br			7.52	7.86	7.68	–0.34	–0.12
28	NOAC					6.70	7.02	7.09	–0.32	–0.39
29	NOAC		$CH{=}CH_2$			7.19	7.36	7.32	–0.20	–0.13
30	NOAC		F			7.05	7.24	7.20	–0.19	–0.15
31	NOAC		Cl			7.77	7.84	7.67	–0.07	0.10
32	NOAC		Br			8.00	7.91	7.89	0.09	0.11
33	NOAC		I			7.89	7.94	8.11	–0.05	–0.22
34	NOAC	Cl	Cl			8.40	7.97	8.26	0.43	0.14
35*	O	F				7.11	6.31	6.86	0.80	0.25
36*	O	NO_2				7.38	7.31	6.36	0.07	1.02
37*	O		Br			7.35	6.85	6.98	0.50	0.37
38*	NOH		F			6.89	7.11	7.01	–0.21	–0.12
39*	NOH	Cl	Cl			8.40	8.39	8.30	0.01	0.10
40*	NOH	CH_3	Br			8.22	8.55	8.38	–0.33	–0.16
41*	NOAC	CH_3	Br			8.15	8.51	8.34	–0.40	–0.19
42*	NOAC	NO_2	Br			8.40	8.24	7.72	0.16	–0.68

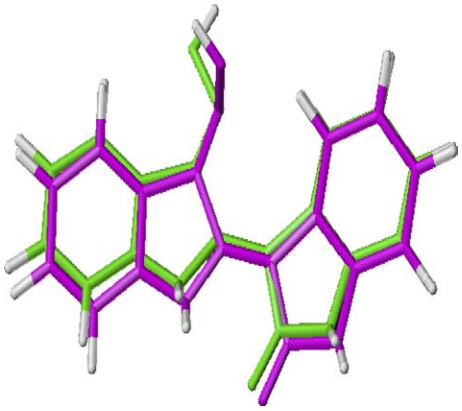

Fig. 1. Superposition of structure extracted from crystal complex (green) and docked structure (magenta).

N1 of the inhibitor, respectively. And Arg141 shields the edge of the inhibitor's aromatic ring from the bulk solvent by orienting its side-chain.

The docking results could give us interaction modes between inhibitors and GSK-3β. The compound **34** was taken as representative to elucidate this point shown in Fig. 2. The hydrogen-bond modes are the same to those observed in the crystal structure of indirubin-3′-oxime complexed with GSK-3, which validates the docking model is reliable. In addition, two aromatic rings of the molecule are placed in the hydrophobic fields by interacting with the side chains of Ala83, Val70, Cys199 and Leu188 of GSK-3β and the chlorine atom at position 6 interacts with Leu132 [20]. The main differences in interaction models of indirubins are different hydrophobic pockets, which shows that hydrophobic interaction is very crucial to the binding of indirubins with GSK-3β.

3.2. CoMFA and CoMSIA models

PLS analysis results are presented in Table 2. The ligand-based CoMFA model has cross-validate coefficient q^2 of 0.790 with five components and conventional r^2 of 0.923, the CoMSIA model with q^2 of 0.780 for seven components and r^2 of 0.916 are obtained. These values indicate that the models are robust.

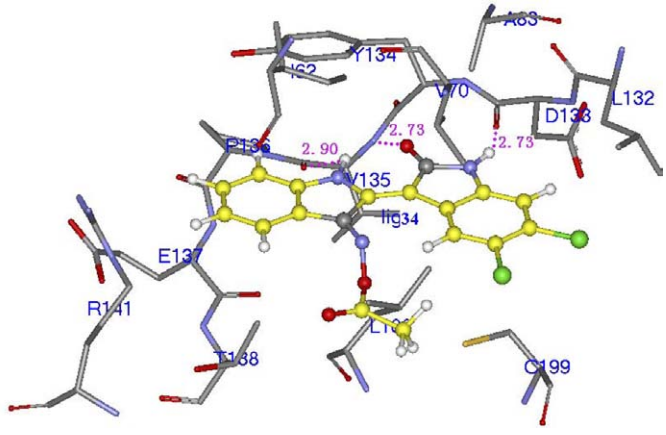

Fig. 2. Interaction models of complex 34-GSK3. Ligand **34** is shown as ball-and stick model with carbon atoms (yellow) and 5.6-2Cl (green), the residues of active pocket are presented in stick. And hydrogen bonds are shown as pink dotted lines with lengths (Å).

The receptor-based CoMFA model has cross-validation coefficient (q^2) of 0.563 and regression coefficient (r^2) of 0.897 for four components. q^2 and r^2 for CoMSIA model are 0.766 and 0.908 with five components using the combination of steric + electric + hydrophobic fields, respectively. The plot of experimental values versus calculated values of CoMSIA model is depicted in Fig. 3. From these values, it seems that the CoMSIA model is better than the CoMFA model. The superiority of CoMSIA might be attributed mainly to high contributions from hydrophobic field, which is not taken into account in CoMFA method.

Ethylene or acetoxime substituent in a few molecules (No. 18 or No. 29) shows different orientation between lower energy conformation and docking conformation. However, no relevant papers report this kind of GSK-3β inhibitors with such substituents, therefore, it is difficult to determine their orientations in real active conformation. From docking results, these substituents extend almost to the outward of binding pocket, which provides more space for side chains to make their conformations change a lot. In addition, these side chains of molecules have little effect on inhibitory activity comparing to their corresponding template without such substituents. Although a little value discrepancy exits in the results obtained from these two methods, conclusions about contour maps distribution of all models are similar and reliable (the ligand-based model figures not shown). The receptor-based CoMSIA model was taken as an example to illustrate factors affecting inhibitory activity, which has a component (**5**) smaller than that of the ligand-based CoMSIA model (**7**).

3.3. Contour map with binding topology

The steric, electrostatic and hydrophobic contour maps with compound **34** as a reference structure combined with residues near the binding pocket of GSK-3β are shown in Fig. 4a, b, respectively. As shown in Fig. 4a, position 5 of indirubins surrounded by green contours locates in a hydrophobic environment near Cys199 and Val70, which means a bulky substituent is helpful for activities. Two yellow regions locating at the left aromatic ring and position 3′ of indirubins represent unfavorable steric effect for inhibitory activities. The residue Arg141 orientates its side-chain to shield the edge of the aromatic ring of indirubins from solvent, makes this site sterically restricted. The bulky group at position 3′ may result in the clash of Gln185 and Asn186. Anyway, adding bulky groups at these two positions is forbidden and decreases affinities between ligands and receptor. Blue and red mean the positive charges being beneficial and detrimental to inhibitory activities, respectively. Position 3′ with blue color is just pointing to the carboxyl of Gln185 which makes positive-rich substituent helpful. The left aromatic rings with negative-rich charges might be helpful to form the π–π interaction with the phenyl of

Table 2
PLS analysis results of CoMFA and CoMSIA models. R-B and L-B means receptor-based and ligand-based, respectively

		N		q^2		r^2	s		Steric	Electrostatic	Hydrophobic
		LOO	LSO	LOO	LSO		calculated	predicted			
R-B	CoMFA	4	3	0.563	0.542	0.897	0.279	0.392	0.543	0.457	
	CoMSIA	5	5	0.766	0.724	0.908	0.268	0.472	0.173	0.391	0.435
L-B	CoMSIA	5	4	0.790	0.757	0.923	0.212	0.380	0.624	0.376	
	CoMFA	7	7	0.780	0.767	0.916	0.261	0.538	0.186	0.401	0.413

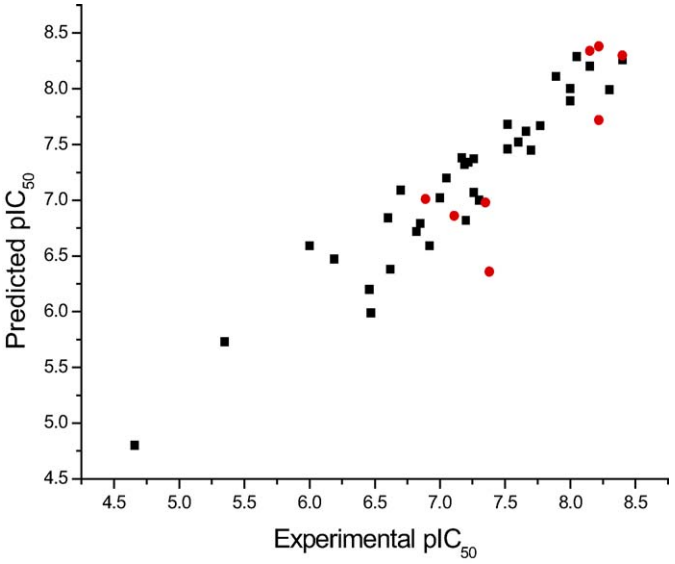

Fig. 3. **CoMSIA** predicted pIC_{50} vs. experimental pIC_{50} values for training set (squares) and test set (circles).

Tyr134. As for the hydrophobic map shown in Fig. 4b, position 6 lies in the cavity of the hydrophobic residues, Val110 and Leu132, so hydrophobicity is preferred (magenta). However, position 6′ (cyan) is close to residues Pro136 and Arg141, and hydrophilic groups may be favored.

4. Conclusion

Both receptor-based and ligand-based methods are appropriate to build 3D-QSAR models of indirubin derivates, models and conclusions derived from two methods are similar and reliable. Factors affecting activity have been elucidated using the representative receptor-based CoMSIA model ($q^2 = 0.766$, $r^2 = 0.908$, N (number of components) = 5 with steric + electric + hydrophobic fields. It illustrates that hydrophobic interactions play an important role in molecules recognition. Factors affecting inhibitory activities are investigated by combing the CoMSIA contour maps with the binding pocket of GSK-3β, and the results are in good accordance and complementary to each other. This would lead to a better understanding of interaction mechanism of indirubins complexed with GSK-3β and might give a rational clue to design more favorable inhibitors of GSK-3.

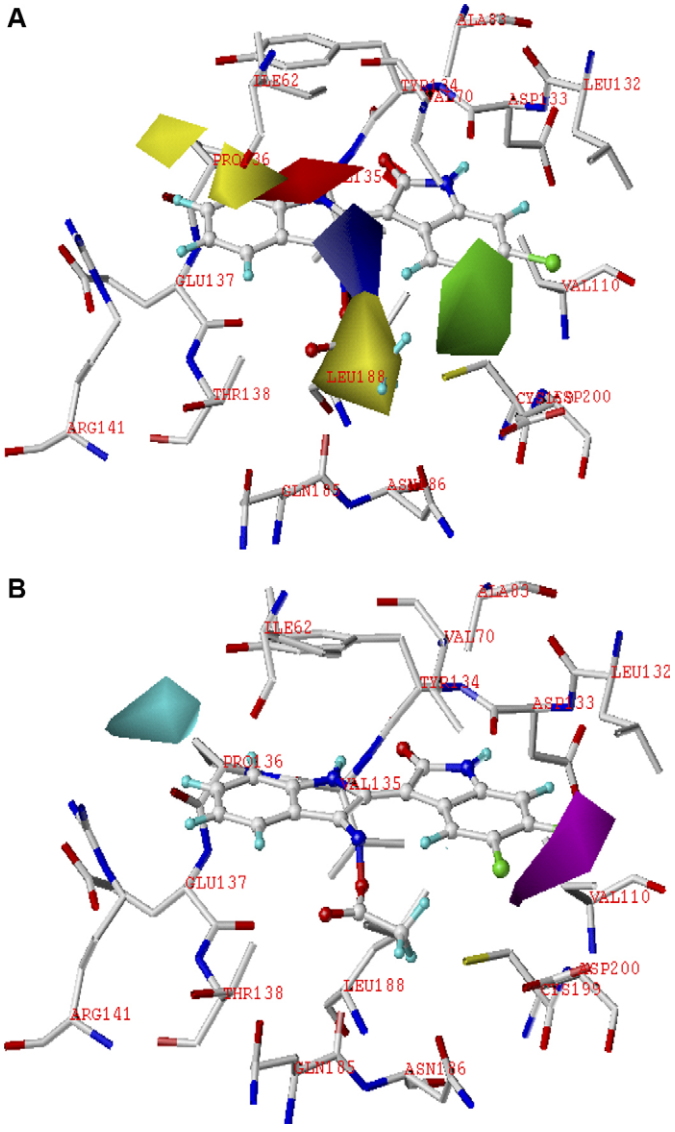

Fig. 4. CoMSIA contour maps combined with the structure topology (residue within 4 Å near the inhibitor 34 without Gln85) of complex 34-GSK3β.
(a) Steric and electrostatic field contribution. Green and yellow means bulky group will increase and decrease inhibitory activity, respectively. Positive and negative potential are favored in blue and red regions, respectively.
(b) Hydrophobic field contribution. Magenta and cyan represent hydrophobic and hydrophilic substituents are helpful to inhibitory activity, respectively.

Acknowledgments

The authors thank professor Arthur J. Olson for his kindness in offering us the AutoDock 3.0.5 program. We are grateful to Doctoral Foundation of Ningbo City, P.R. China for financial support (Nos. 2004A610010, 2004A610018) and Ningbo Online Technology Market and Cooperation Project (2004A410049).

References

[1] J.R. Woodgett, EMBO J. 9 (1990) 2431–2438.
[2] J.R. Wood, Methods Enzymol. 200 (1991) 564–577.
[3] K.P. Ali, J.R. Hoeflich, Woodgett, Chem. Rev. 101 (2001) 2527–2540.
[4] W. Doble, J.R. Woodgett, J. Cell Sci. 116 (2003) 1175–1186.
[5] A.S. Wagman, K.W. Johnson, D.E. Bussiere, Curr. Pharm. Des. 10 (2004) 1105–1137.
[6] A. Martinez, A. Castro, I. Dorronsoro, M. Alonso, Med. Res. Rev. 22 (2002) 373–384.
[7] C. Kunick, K. Lauenroth, K. Wieking, X. Xie, S. Christiane, et al., J. Med. Chem. 47 (2004) 22–36.
[8] E. Lescot, R. Bureau, J. Sopkova-de Oliveira Santos, R. Christophe, L. Vincent, J.C. Lancelot, S. Rault, J. Chem. Inf. Model. 45 (2005) 708–715.
[9] M. Zeng, Y.J. Jiang, B. Zhang, K.W. Zheng, N. Zhang, Q.S. Yu, Bioorg. Med. Chem. Lett. 15 (2005) 395–399.
[10] W. Tang, G. Eisenbrand, Chinese Drugs of Plant Origin: Chemistry, Pharmacology, and Use in Traditional and Modern Medicine, Springer-Verlag, Heidelberg, 1998.
[11] S. Leclerc, M. Garnier, R. Hoessel, D. Marko, J.A. Bibb, G.L. Snyder, et al., J. Biol. Chem 276 (2001) 251–260.
[12] P. Bernard, M. Pintore, J.-Y. Berthon, J.R. Chrétien, Eur. J. Med. Chem. 36 (2001) 1–19.
[13] J.K. Olamwini, H. Assefa, J. Med. Chem. 45 (2002) 841–852.
[14] A.M. de Oliveira, F.B. Custo´dio, C.L. Donnici, C.A. Montanari, Eur. J. Med. Chem. 38 (2003) 141–155.
[15] BiomedCache version 6.0; Beaverton, Fujitsu America Inc. 2003.
[16] Sybyl Version 6.8; St. Louis (MO), Tripos Associates Inc., 2001.
[17] P. Polychronopoulos, P. Magiatis, A.-L. Skaltsounis, V. Myrianthopoulos, E. Mikros, A. Tarricone, A. Musacchio, S.M. Roe, L. Pearl, M. Leost, P. Greengard, L. Meijer, J. Med. Chem. 47 (2004) 935–946.
[18] G.M. Morris, D.S. Goodsell, R. Huey, W.E. Hart, S. Halliday, R. Belew, A.J. Olson, Autodock Version 3.05 user manual 2000.
[19] J.A. Bertrand, S. Thieffine, A. Vulpetti, C. Cristiani, B. Valsasina, S. Knapp, H.M. Kalisz, et al., J. Mol. Biol. 333 (2003) 393–407.
[20] L. Meijer, A.-L. Skaltsounis, P. Magiatis, P. Polychronopoulos, et al., Chem & Bio. 10 (2003) 1255–1266.